

# Phenomenological signatures of mixed complex scalar WIMP dark matter

Mitsuru Kakizaki,<sup>1,\*</sup> Akiteru Santa,<sup>1,†</sup> and Osamu Seto<sup>2,3,4,‡</sup>

<sup>1</sup> *Department of Physics, University of Toyama,  
3190 Gofuku, Toyama 930-8555, Japan*

<sup>2</sup> *Office of International Affairs, Hokkaido University, Sapporo 060-0815, Japan*

<sup>3</sup> *Department of Physics, Graduate School of Science,  
Hokkaido University, Sapporo 060-0810, Japan*

<sup>4</sup> *Department of Life Science and Technology,  
Hokkai-Gakuen University, Sapporo 062-8605, Japan*

## Abstract

We discuss phenomenological aspects of models whose scalar sector is extended by an isospin doublet scalar and a complex singlet scalar as an effective theory of supersymmetric models with mixed sneutrinos. In such models, the lighter of the mixed neutral scalars can become a viable dark matter candidate by imposing a global  $U(1)$  symmetry. We find that the thermal WIMP scenario is consistent with the cosmological dark matter abundance when the mass of the scalar is half of that of the discovered Higgs boson or larger than around 100 GeV. We also point out that, with an additional isospin singlet Majorana fermion mediator, even the mass of the scalar WIMP less than around 5 GeV is compatible with the observed dark matter abundance. We show that such cosmologically allowed regions can be explored at future collider experiments and dark matter detections.

---

\*Electronic address: kakizaki@sci.u-toyama.ac.jp

†Electronic address: santa@jodo.sci.u-toyama.ac.jp

‡Electronic address: seto@particle.sci.hokudai.ac.jp

## I. INTRODUCTION

The discovery of the Higgs boson with a mass of 125 GeV [1, 2] and measurements of its properties at the CERN Large Hadron Collider (LHC) have established the Higgs mechanism, on which the Standard Model (SM) of particle physics is based. Although no clear evidence against the SM has been found at collider experiments, several phenomena that necessitate a new theory underlying the SM have been reported mainly from the cosmological and astrophysical observations. These include the existence of dark matter (DM), the baryon asymmetry of the Universe, the cosmic inflation as well as neutrino oscillations. We are obliged to build new models beyond the SM and to develop methods for distinguishing them in order to approach the fundamental theory.

Weakly Interacting Massive Particles (WIMPs)  $\chi$  are ones of the most promising candidates for the DM in our Universe, whose abundance is determined to be  $\Omega h^2 = 0.1$  by the data obtained at the WMAP [3] and Planck observations [4]. If the thermal relic abundance of the WIMPs coincides with the observed value above, the energy scale of the new model containing the WIMP is set at around the terascale. Therefore, WIMP models can be explored by using data obtained at the operative LHC Run-II and the future electron-positron colliders, such as International Linear Collider (ILC) [5–8], the Compact Linear Collider (CLIC) [9] and the Future Circular Collider of electrons and positrons (FCC-ee) [10], as well as many DM direct and indirect detection experiments.

Let us take a closer look at the nature of WIMPs. As suggested by its name, WIMPs appear to have the weak interactions with other SM particles. However, such WIMPs that couple with the  $Z$ -boson have too large annihilation cross sections and scattering cross sections with nuclei. The latter property completely conflicts with the null results of direct DM search experiments, hence the coupling between the WIMP and the  $Z$ -boson should be absent or strongly suppressed. For Majorana WIMPs with the  $SU(2)$  gauge interaction, the coupling with the  $Z$ -boson does not exist. For scalar WIMPs, similarly, introduction of a  $CP$  violating term in the scalar potential removes the coupling with the  $Z$ -boson. Such a prescription is common in order to avoid the direct DM search constraints in the literature, for example, in the inert doublet scalar model [11, 12]. On the contrary,  $SU(2)$  singlet WIMPs, by definition, do not interact with the  $Z$ -boson. Thus, small scattering cross sections with nuclei are predicted, and the direct DM search limit has been relatively easily

avoided. As one of the simplest models, singlet scalar DM models have been intensively investigated as the operator between real singlet scalar WIMP and the SM Higgs doublet  $H$ ,  $\mathcal{O} = \lambda_{H\chi}|H|^2\chi^2$ , is allowed by renormalizability [13–15]. Nevertheless, due to recent great progress in direct DM search experiments, significant constraints on the coupling  $\lambda_{H\chi}$  have been imposed even for singlet DM. On the other hand, small  $\lambda_{H\chi}$  allowed by the direct detection constraints leads to the overabundance of the WIMP DM if one relies on the thermal WIMP paradigm mentioned above. From the above observations about the WIMP coupling with (without) the  $Z$ -boson,  $SU(2)$  doublet (singlet) WIMPs end up with under-(over-)abundance in the Universe [16]. Therefore, one can envisage that doublet-singlet mixed WIMPs may have the correct relic abundance and be consistent with the current direct DM search results simultaneously for CP-conserving scalar or Dirac fermion DM cases in, *e.g.*, Ref. [17]<sup>1</sup>. For example, a supersymmetric (SUSY) model in which left-handed and right-handed sneutrinos significantly mix due to the large sneutrino trilinear coupling falls in this category [16, 18–21].

In this Paper, we investigate the phenomenology of scalar-type doublet-singlet mixed DM models as simplified models of the mixed sneutrino DM models: Since the quantum numbers of the introduced scalar doublet (singlet) in this Paper is the same as those of the left-handed sleptons (right-handed sneutrinos), the mixed sneutrino models are reduced to our model if all the other superparticles decouple and SUSY relations among couplings are relaxed. Hence, while our model is strongly motivated by the mixed sneutrino models, differences that stem from the absence of SUSY relations among couplings can also be easily found by comparing the results of this Paper with those of previous studies on mixed sneutrino models. We examine the parameter space consistent with the cosmological DM abundance. The allowed regions are found when the mass of the WIMP is half of that of the Higgs boson or larger than around 100 GeV. If we further introduce a Majorana mediator that corresponds to the bino in the mixed sneutrino models, the mass of the thermal WIMP can be lighter than around 5 GeV. Then, we discuss phenomenological implications for future collider experiments and DM detection experiments.

---

<sup>1</sup> Doublet-singlet Majorana WIMP models have been investigated in, *e.g.*, Refs. [22, 23]. In , *e.g.*, Refs. [22, 24–27], doublet-singlet mixed real scalar WIMP models with an additional  $Z_2$  symmetry also have been studied. Mixed complex scalar WIMP scenarios we focus on are qualitatively different from such CP-violating scalar or Majorana fermion WIMP scenarios.

TABLE I: The quantum numbers of the electroweak fields in the mixed complex scalar WIMP model.

Fields	$SU(3)_C$	$SU(2)_L$	$U(1)_Y$	$U(1)_X$
Left-handed lepton doublets ( $L_i$ )	<b>1</b>	<b>2</b>	$-1/2$	0
Right-handed lepton singlets ( $e_i$ )	<b>1</b>	<b>1</b>	$-1$	0
SM Higgs doublet ( $H$ )	<b>1</b>	<b>2</b>	$+1/2$	0
Inert scalar doublet ( $\eta$ )	<b>1</b>	<b>2</b>	$+1/2$	+1
Inert scalar singlet ( $s$ )	<b>1</b>	<b>1</b>	0	+1

This paper is organized as follows. We introduce our model in the Sec. II. After summarizing all constraints on the model in Sec. III, we show its phenomenological implications in Sec. IV. In Sec. V, our model is extended by a light Majorana mediator for enhancing the WIMP annihilation. We show phenomenological consequences also for the new viable parameter region. Section VI is devoted to concluding remarks.

## II. THE MODEL

We introduce a complex scalar isospin doublet  $\eta$  and singlet  $s$  in addition to the SM particle contents. These new fields,  $s$  and  $\eta$ , are charged under a new global  $U(1)_X$  symmetry. The SM Higgs doublet  $H$  is neutral under the  $U(1)_X$  symmetry. The quantum numbers of the electroweak fields above are listed in Table I. The  $U(1)_X$  charge corresponds to the dark matter number, and the  $U(1)_X$  symmetry guarantees the stability of the lightest additional particle. Then, the scalar potential allowed by the  $SU(3)_C \otimes SU(2)_L \otimes U(1)_Y \otimes U(1)_X$  symmetries and renormalizability is written as

$$\begin{aligned}
 V = & \mu_H^2(H^\dagger H) + \frac{\lambda_1}{2}(H^\dagger H)^2 + \mu_\eta^2(\eta^\dagger \eta) + \frac{\lambda_2}{2}(\eta^\dagger \eta)^2 + \lambda_3(H^\dagger H)(\eta^\dagger \eta) + \lambda_4(H^\dagger \eta)(\eta^\dagger H) \\
 & + \mu_s^2(s^* s) + \frac{\lambda_s}{2}(s^* s)^2 + \lambda_{Hs}(H^\dagger H)(s^* s) + \lambda_{\eta s}(\eta^\dagger \eta)(s^* s) + A(\eta^\dagger H s + \text{h.c.}), \quad (1)
 \end{aligned}$$

where  $\mu^2$ 's,  $\lambda$ 's and  $A$  are mass and coupling parameters. It should be noticed that, because of the  $U(1)_X$  symmetry, the scalar potential does not contain the  $CP$  violating operator,  $\mathcal{O} = \lambda_5(H^\dagger \eta)^2 + \text{h.c.}$ , which is usually considered in the two Higgs doublet models.

After the electroweak symmetry breaking, the neutral component of the SM Higgs doublet develops a vacuum expectation value,  $\langle H^0 \rangle = v/\sqrt{2}$ , with  $v = 246$  GeV. Then, the mass

squared matrix of the neutral component of the inert doublet  $\eta^0$  and the inert singlet  $s$  in the  $(\eta^0, s)$  basis is diagonalized as

$$\begin{aligned} \begin{pmatrix} m_{11}^2 & m_{12}^2 \\ m_{21}^2 & m_{22}^2 \end{pmatrix} &\equiv \begin{pmatrix} \mu_\eta^2 + \frac{v^2}{2}\lambda & \frac{v}{\sqrt{2}}A \\ \frac{v}{\sqrt{2}}A & \mu_s^2 + \frac{v^2}{2}\lambda_{Hs} \end{pmatrix} \\ &= \begin{pmatrix} \cos\theta_\chi & -\sin\theta_\chi \\ \sin\theta_\chi & \cos\theta_\chi \end{pmatrix} \begin{pmatrix} m_{\chi_2}^2 & 0 \\ 0 & m_{\chi_1}^2 \end{pmatrix} \begin{pmatrix} \cos\theta_\chi & \sin\theta_\chi \\ -\sin\theta_\chi & \cos\theta_\chi \end{pmatrix}, \end{aligned} \quad (2)$$

with  $\lambda \equiv \lambda_3 + \lambda_4$ . The mass eigenvalues and the mixing angle satisfy  $m_{\chi_1} < m_{\chi_2}$  and  $-\pi/2 < \theta_\chi < \pi/2$ . The lighter state  $\chi_1$  is stable and identified with the WIMP candidate in our model. The masses of the charged components  $\eta^\pm$  are given by

$$m_{\eta^\pm}^2 = \mu_\eta^2 + \frac{v^2}{2}\lambda_3. \quad (3)$$

Ones of the most important interactions of the WIMP  $\chi_1$  in our analysis are the couplings to the  $Z$ -boson and to the SM Higgs boson  $h$ , which depend on the mixing angle  $\theta_\chi$  as

$$\mathcal{L} \supset -i \frac{e}{\sin 2\theta_W} \sin^2 \theta_\chi (\chi_1^* \overleftrightarrow{\partial}_\mu \chi_1) Z^\mu + \left( -v\lambda \sin^2 \theta_\chi - v\lambda_{Hs} \cos^2 \theta_\chi + \frac{A}{\sqrt{2}} \sin 2\theta_\chi \right) h \chi_1^* \chi_1. \quad (4)$$

### III. EXPERIMENTAL CONSTRAINTS

Here we discuss experimental constraints on the parameter space of our model. In the framework of the standard thermal WIMP production scenario, the DM abundance as well as direct and indirect DM detection results impose significant constraints on the WIMP properties. Null results of collider searches for new particles also considerably constrain the model parameter space. We list notable experimental bounds adopted in our analysis in Table II, and describe them below.

The DM relic density  $\Omega h^2$  is determined through cosmological observations, most notably by WMAP [3] and Planck [4]. Taking the possibility that nonthermal WIMP production contributes to the WIMP abundance into account, we consider the value of  $\Omega h^2$  shown in Table II as the upper limit of the thermal WIMP abundance. The thermal WIMP abundance is controlled by WIMP annihilation cross sections. In most of the parameter region of this inert scalar model, dominant WIMP annihilation modes are  $\chi_1 \chi_1^* \rightarrow b\bar{b}$  and  $\chi_1 \chi_1^* \rightarrow W^+ W^-$

TABLE II: The experimental bounds adopted in our analysis.

Observable	Experimental bound
$\Omega h^2$	$0.1196 \pm 0.0062$ (95% CL) [4]
$\sigma_{\text{Nucleon}}$	LUX [28, 29], CDMSlite [30]
$\langle \sigma_{\text{ann}} v \rangle$	Fermi-LAT [31–33]
$\Gamma(Z \rightarrow \text{inv.})$	$< 2.0$ MeV (95% CL) [34]
$\text{Br}(h \rightarrow \text{inv.})$	$< 0.23$ (95% CL) [35, 36]

processes. This argument puts the lower bound to the mixing angle  $\theta_\chi$ . We also explore parameter regions where coannihilation processes become important.

Direct DM detection experiments search for signals by the recoil energy through WIMP scattering off nuclei. With null results, the expected number of events by WIMPs in each experiment set the upper bound on the scattering cross section of the WIMP with a nucleon  $\sigma_{\text{Nucleon}}$ . For a WIMP with a mass of the order of  $\mathcal{O}(100)$  GeV, recent results obtained at the LUX experiment constrain the WIMP-nucleon cross section as  $\sigma_{\text{Nucleon}} \lesssim \mathcal{O}(10^{-46})$  cm<sup>2</sup> [29]. For a WIMP with a mass around 5 GeV, the CDMSlite experiment imposes the most stringent upper limit as  $\sigma_{\text{Nucleon}} \lesssim \mathcal{O}(10^{-41})$  cm<sup>2</sup> [30]. In our model, the spin independent cross section of  $\chi_1$  is mediated by the Higgs boson and  $Z$ -boson.

The measurements of fluxes of various cosmic rays serve as indirect DM searches. The most stringent limit on the DM annihilation cross section has been obtained from diffuse  $\gamma$ -ray flux from dwarf spheroidal galaxies by Fermi-LAT [31, 32]. No  $\gamma$ -ray signal from DM annihilation in the Small Magellanic Cloud puts a similar bound on the WIMP annihilation cross section [33]. In addition, Super-Kamiokande results can impose upper limits on WIMP-nucleon scattering cross sections by non-observation of neutrinos from WIMP annihilation in the Sun [37], which might be important for WIMPs with a mass less than around 10 GeV. However, those indirect search constraints are not so stringent as others. Therefore, these indirect search limits do not explicitly appear in our later plots although we take them into account.

Let us turn to constraints obtained from collider experiments. If the mass of  $\chi_1$  is smaller than half of the mass of the  $Z$ -boson (the discovered Higgs boson), the  $Z$ -boson (the Higgs boson) can decay invisibly into a pair of  $\chi_1$ . The invisible decays of the  $Z$ - and Higgs bosons have been searched for at LEP [34] and LHC [35, 36]. Since these decay widths

are proportional to  $\sin^4 \theta_\chi$ , the null results impose the upper limit on  $\sin \theta_\chi$ . Moreover, collider experiments set bounds on the masses and couplings of yet-to-be-discovered particles through processes associated with WIMPs. For example, if the charged inert scalars  $\eta^\pm$  are once produced, they decay into  $W^{\pm(*)}$  and the missing  $\chi_1$ . From Eqs. (2) and (3), the squared mass difference for small mixing angle,  $\theta_\chi \ll 1$ , is given by  $m_{\chi_2}^2 - m_\eta^2 \simeq v^2 \lambda_4 / 2$ . In our analysis, the reference value of  $\lambda_4$  is as small as the corresponding scalar coupling constant derived from the SU(2) D-terms in the mixed sneutrino models [16, 18–21] as  $\lambda_4 = 2m_Z^2 \cos^2 \theta_W \cos^2 \beta / v^2 \simeq 2.3 \times 10^{-5}$  with  $\tan \beta = 10$ . Therefore, the charged and heavy neutral scalars are sufficiently degenerate in mass, leading to negligible contributions to the  $T$  parameter,  $\Delta T \sim 0$ .

#### IV. NUMERICAL RESULTS

With the aid of LanHEP [38], which automatically generates Feynman rules, we implement our mixed complex scalar WIMP model into the public codes `micrOMEGAs` [39] and `CalcHEP` [40], which allows for automated computations of the properties of DM and associated new particles. All numerical results presented here are obtained with `micrOMEGAs` and `CalcHEP`. As benchmark scenarios in our analysis, we take the scan bounds and reference values listed in Table III. It should be noticed that the  $h\chi_1\chi_1^*$ -coupling given in Eq. (4) controls both the WIMP-nucleon scattering cross section and annihilation cross sections. Thus, the effect of the variation of  $\lambda$  or  $\lambda_{H_s}$  can be absorbed by the change of the third term, and thus the viable mass range of  $\chi_1$  is not altered. Moreover, the first term in the  $h\chi_1\chi_1^*$ -coupling is strongly suppressed by  $\sin^2 \theta_\chi$ , and thus negligible in many cases. From this observation, we fix the values of the parameters  $\lambda$  and  $\lambda_{H_s}$  at those motivated in the mixed sneutrino WIMP scenarios [16, 18–21], where  $\lambda = (m_Z^2/v^2) \cos 2\beta$  and  $\lambda_{H_s} = |y_\nu|^2 \simeq 0$ . In the small  $\theta_\chi$  limit with finite  $\lambda_{H_s}$ , the second term of  $h\chi_1\chi_1^*$ -coupling in Eq. (4) becomes the most relevant, hence this model is reduced to the so-called Higgs portal singlet scalar DM model. For  $\tan \beta = 10$ , we obtain  $\lambda = -0.14$ . Given the experimental constraints discussed in the previous section, we find two classes of allowed parameter region: (A)  $m_{\chi_1} \simeq m_h/2$  (Higgs-pole region); and (B)  $m_{\chi_1} \gtrsim 100$  GeV (Large WIMP mass region).

TABLE III: The scan bounds and reference values of parameters of our model.

Parameter	Scan bound / Reference value
$m_{\chi_1}$	[10 MeV, 1.5 TeV]
$m_{\chi_2}$	[100 GeV, 16.5 TeV]
$\sin \theta_\chi$	[0.001, 1]
$m_\psi$	[10 MeV, 1.01 TeV]
$\lambda$	-0.14
$\lambda_{Hs}$	0

### A. Higgs-pole region

A viable parameter region can be found when the WIMP annihilation in the early Universe takes place near the Higgs pole, namely  $m_{\chi_1} \simeq m_h/2$ . Figure 1 shows experimental constraints and future prospects in the  $(m_{\chi_2}, \sin \theta_\chi)$  plane for  $m_{\chi_1} = 62$  GeV. Excluded parameter regions in the light of current experimental bounds are shown with mesh areas. In the red mesh region, the resultant relic abundance exceeds the observed DM density [4]. The green mesh region is excluded by the LUX experiment [29]. The purple solid line indicates the expected reach by the XENON-1T experiment [41].

The WIMP-nucleon scattering is induced mainly by the  $Z$ -boson exchange diagram for  $m_{\chi_2} \lesssim 1000$  GeV, and by the Higgs boson one for  $m_{\chi_2} \gtrsim 1000$  GeV. This fact leads to the break of the direct detection limit around  $m_{\chi_2} \simeq 1000$  GeV in Fig. 1. Since  $m_{\chi_1} \simeq m_h/2$ , the  $s$ -channel Higgs boson exchange process is the dominant annihilation mode and controls the relic density. For this process, the most relevant interaction is the third term of  $h\chi_1\chi_1^*$ -coupling in Eq. (4), which is rewritten as

$$\frac{A}{\sqrt{2}} \sin 2\theta_\chi \simeq \frac{\sin^2 2\theta_\chi (m_{\chi_2}^2 - m_{\chi_1}^2)}{2v}. \quad (5)$$

Namely, a larger mass difference between  $\chi_1$  and  $\chi_2$  leads to a smaller relic density, resulting in a viable region for  $m_{\chi_2} \gtrsim 1000$  GeV. As can be seen from Fig. 1, the current allowed region can be ruled out by the XENON-1T experiment.

We comment on the vacuum stability bound. Since the trilinear coupling  $A$  is large in the allowed Higgs-pole region, there may appear a deeper vacuum than the electroweak one. In Ref. [20], vacuum meta-stability has been investigated in mixed sneutrino WIMP scenarios.



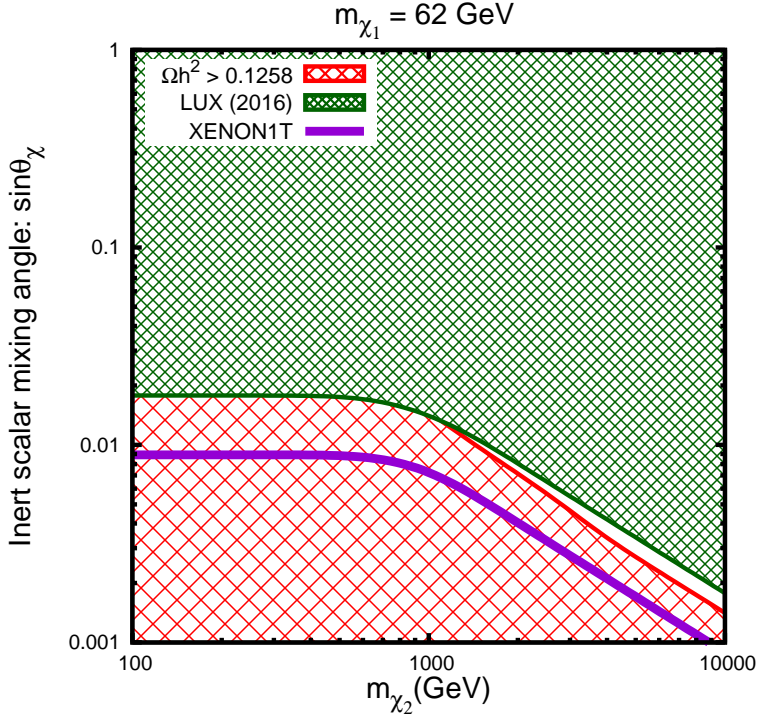


FIG. 1: Experimental constraints and future prospects in the  $(m_{\chi_2}, \sin\theta_\chi)$  plane in the complex scalar for  $m_{\chi_1} = 62$  GeV.

It has been shown that the upper bound on the mixing angle is  $\sin\theta_\nu \lesssim 0.26$  for a WIMP mass of  $m_{\tilde{\nu}} \sim 1$  GeV. Since in our model the mixing angle in the allowed Higgs-pole region is as small as  $\sin\theta_\chi \lesssim 0.01$ , we expect that the electroweak vacuum is stable enough. Further discussion on the vacuum stability is beyond the scope of this paper.

## B. Large WIMP mass region

Constraints from direct DM searches become weaker as the WIMP mass is increased for  $m_{\chi_1} \gtrsim 100$  GeV, leading to another viable mass region. Figure 2 shows allowed regions in such large WIMP mass cases in the  $(m_{\chi_1}, \sin\theta_\chi)$  plane. There are two representative cases for decreasing the WIMP relic abundance for  $m_{\chi_1} \gtrsim 100$  GeV: The masses of  $\chi_1$  and  $\chi_2$  are considerably split, or degenerate enough to coannihilate. In the split case, the mass difference between  $\chi_1$  and  $\chi_2$  should be large so that the WIMP coupling to the Higgs boson and the annihilation cross section are sufficiently enhanced. In our numerical analysis, we take  $(m_{\chi_2} - m_{\chi_1})/m_{\chi_1} = 10$  for the split case, and  $(m_{\chi_2} - m_{\chi_1})/m_{\chi_1} = 0.01$  for the

degenerate case. In this degenerate case, the charged scalar decays into  $\chi_1$  and too soft jets or leptons to be detected. Therefore, the charged scalar mass  $m_{\eta^\pm}$  is not constrained at the LHC. The dominant coannihilation modes of  $\eta^+\eta^- \rightarrow W^+W^-$ ,  $\chi_2\chi_2 \rightarrow W^+W^-(ZZ)$  and  $\chi_2\eta^\pm \rightarrow \gamma W^\pm$  significantly decrease the WIMP relic abundance. These modes contribute to around 30% of the effective annihilation cross section. As one can see from Fig. 2, the viable parameter region in the split case (top frame) lies in the reach of the future XENON-1T experiment. On the other hand, that in the degenerate case (bottom) is only partially covered by the expected XENON-1T sensitivity reach. Therefore, these two cases are distinguishable through future direct detection experiments.

## V. THE MODEL WITH A MAJORANA FERMION

In the previous section, we have shown that there are two regions consistent with current experimental results in our mixed complex scalar WIMP model; the Higgs-pole region where  $m_{\chi_1} \simeq m_h/2$  and large WIMP mass region where  $m_{\chi_1} \gtrsim \mathcal{O}(10^2)$  GeV. Thus, a mass of around 60 GeV appears to be the smallest for viable mixed complex scalar WIMPs. However, in fact, a minor extension of the model opens another viable mass range. In this section, we show that a GeV-mass WIMP is also feasible by introducing only one light Majorana fermion  $\psi$  that mediates WIMP annihilation into the model described in Sec. II.

We assume that the newly introduced Majorana fermion is totally singlet under all the SM gauge symmetry as well as the global  $U(1)_X$  symmetry. The quantum numbers of the electroweak particles of this new model is summarized in Table IV. The left- and right-handed leptons,  $L_i$  and  $e_i$ , have negative  $U(1)_X$  charges in this model. Here,  $i$  ( $= 1 - 3$ ) denotes the generation index. Then, interaction terms among the inert doublet, the left-handed lepton doublets and the Majorana fermion are allowed with their couplings dependent on the lepton generations. Assuming a hierarchical relation in these couplings, we introduce only the interaction with the third generation left-handed lepton as

$$\Delta\mathcal{L} = -Y (\bar{L}_3\psi\tilde{\eta} + \text{h.c.}), \quad (6)$$

with  $Y$  being a Yukawa coupling constant, and  $\tilde{\eta} = i\sigma_2\eta^*$ , where  $\sigma_2$  is the second Pauli

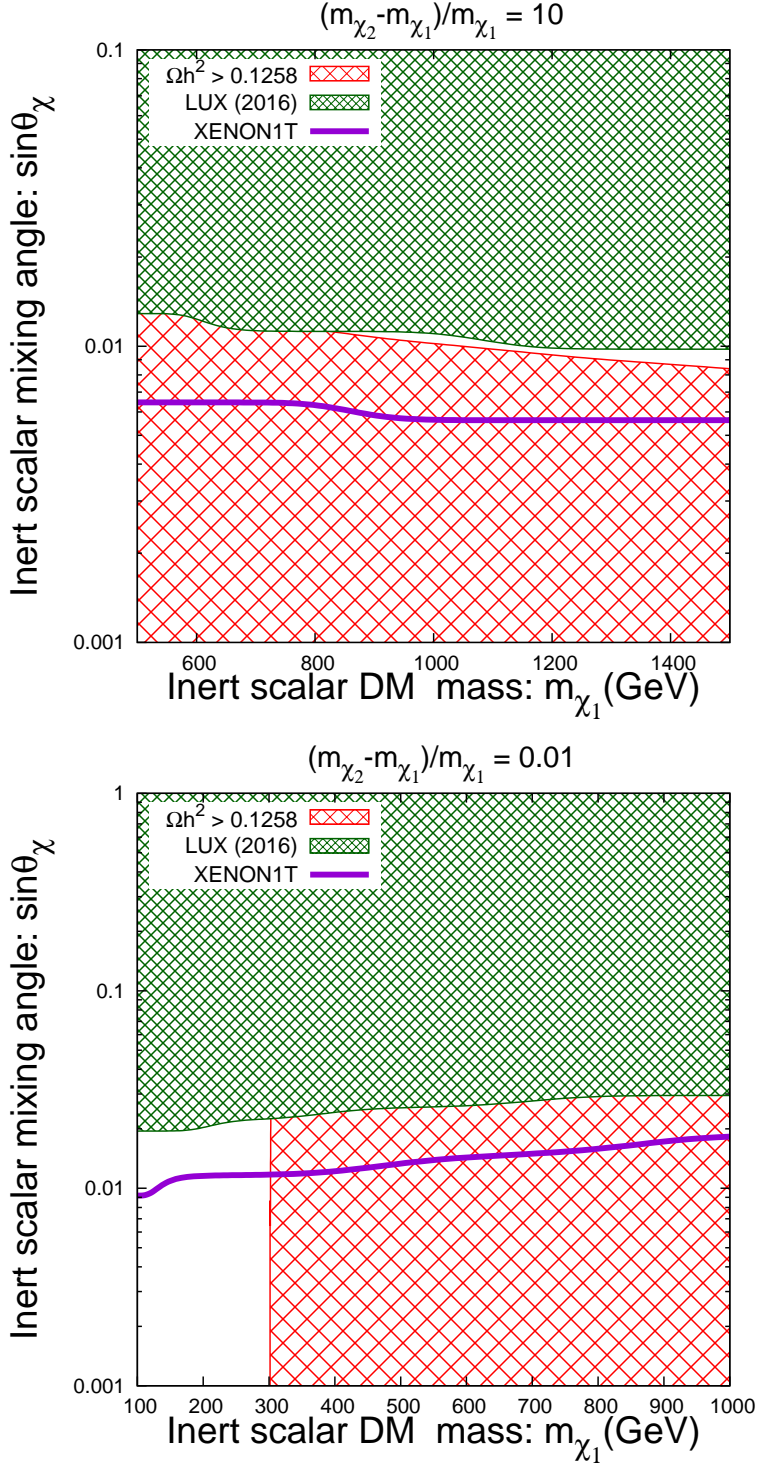


FIG. 2: Experimental constraints and future prospects in the  $(m_{\chi_1}, \sin\theta_\chi)$  plane in the mixed complex scalar WIMP model. The top (bottom) frame shows the split (degenerate) case for  $(m_{\chi_2} - m_{\chi_1})/m_{\chi_1} = 10$  ( $(m_{\chi_2} - m_{\chi_1})/m_{\chi_1} = 0.01$ ).

TABLE IV: The quantum numbers of the electroweak particles in the mixed complex scalar WIMP model with a Majorana fermion.

	$SU(3)_C$	$SU(2)_L$	$U(1)_Y$	$U(1)_X$
Left-handed lepton ( $L_i$ )	<b>1</b>	<b>2</b>	$-1/2$	$-1$
Right-handed lepton ( $e_i$ )	<b>1</b>	<b>1</b>	$-1$	$-1$
SM Higgs doublet ( $H$ )	<b>1</b>	<b>2</b>	$+1/2$	$0$
Inert scalar doublet ( $\eta$ )	<b>1</b>	<b>2</b>	$+1/2$	$+1$
Inert scalar singlet ( $s$ )	<b>1</b>	<b>1</b>	$0$	$+1$
Majorana fermion ( $\psi$ )	<b>1</b>	<b>1</b>	$0$	$0$

matrix. In the mass eigenstates, this interaction is expressed as

$$\Delta\mathcal{L} = \frac{Y}{2} \sin\theta_\chi [\bar{\nu}_\tau(1 - \gamma_5)\psi\chi_1^* + \text{h.c.}] + \dots \quad (7)$$

The bottom line is that with this additional interaction, GeV-mass WIMPs can annihilate into a pair of anti-tau neutrinos through the  $t$ -channel  $\psi$  exchange,  $\chi_1\chi_1 \rightarrow \bar{\nu}_\tau\bar{\nu}_\tau$ . The annihilation modes into fermion and anti-fermion pairs,  $\chi_1\chi_1^* \rightarrow f\bar{f}$ , contribute to the effective annihilation cross section less than 1%. Since  $\psi$  is an isospin singlet, the invisible decay widths of the  $Z$ - and Higgs bosons to a pair of  $\psi$  are absent due to the  $SU(2)$  invariance.

### A. Experimental constraints

The experimental constraints described in Sec. III also apply to the new WIMP model with a Majorana mediator. In addition, the existence of the new decay modes  $\eta^\pm \rightarrow \tau^\pm\psi$ , which are induced by the Yukawa interaction in Eq.(6), imposes another constraint on  $\eta^\pm$ . It should be noticed that similar processes are analyzed in the context of SUSY models. Non-observation of signals of two leptons plus a missing energy sets bounds on slepton masses [42–45]. Searches for the stau  $\tilde{\tau}$  through the decay into the lightest neutralino  $\tilde{\chi}^0$ ,  $\tilde{\tau} \rightarrow \tau\tilde{\chi}_1^0$ , at the LHC experiment impose the lower limit on the mass of the stau as [45]

$$m_{\tilde{\tau}_L} > 93.1 \text{ GeV} \quad (95\% \text{ CL}), \quad (8)$$

for a massless neutralino. For simplicity, we apply this bound on the mass of the charged inert scalar  $\eta^\pm$  in our model.

## B. Numerical results

Our numerical results in the model with the Majorana mediator are shown in Fig. 3 for  $m_{\chi_1} < 10$  GeV and in Fig. 4 for  $100 \text{ GeV} < m_{\chi_1} < 1000$  GeV.

In Fig. 3, experimental constraints and future prospects are shown in the  $(m_{\chi_1}, \sin\theta_\chi)$  plane for  $m_{\chi_2} = 130$  GeV,  $(m_\psi - m_{\chi_1})/m_{\chi_1} = 0.2$  and  $Y = 1$ . The blue hatched region is excluded by the null results of the invisible decay of the Higgs boson at the LHC [35, 36]. The region where the thermal WIMP abundance is overabundant is covered with red mesh [4]. The excluded regions by the CDMSlite experiment [30] and LUX experiments [28] are covered with magenta mesh and green mesh, respectively. The solid purple line shows the future expected sensitivity of SuperCDMS SNOLAB [46]. The solid (dashed) black line represents the case where the invisible decay rate of the Higgs boson is  $\text{Br}(h \rightarrow \text{inv.}) = 0.01$  (0.005). These values should be compared with the future expected sensitivity at the ILC. The ILC stage with  $\sqrt{s} = 250$  GeV and  $L = 250 \text{ fb}^{-1}$  aims the level of  $\text{Br}(h \rightarrow \text{inv.}) = 0.0069$  using the polarization configuration of  $(P_{e^-}, P_{e^+}) = (+80\%, -30\%)$  [47]. In our numerical calculations, we take  $m_{\chi_2} = 130$  GeV so that the Higgs boson does not decay into states containing invisible  $\chi_2$ . WIMP annihilation proceeds not only by the Higgs boson or the  $Z$ -boson but also by the  $t$ -channel exchange of  $\psi$ , and the resultant relic abundance depends on the mass and the coupling of the Majorana mediator. We find that the effective annihilation cross section (the relic abundance) is maximized (minimized) for  $(m_\psi - m_{\chi_1})/m_{\chi_1} = 0.2$ . For smaller mass differences, coannihilation effects rather increase the relic abundance. As for the Yukawa coupling, we set  $Y = 1$  as a reference. Larger  $Y$  relaxes the constraint from the DM relic abundance, and vice versa. For  $m_{\chi_1} < 5$  GeV, the LHC imposes the strongest limit on the mixing angle as  $\sin\theta_\chi < 0.14$ . This figure shows that the allowed region can be further explored by future DM direct detection and precise measurements of the invisible decay of the Higgs boson at future electron-positron colliders.

The introduction of the Majorana mediator also affects the allowed region for large WIMP mass cases as shown in Fig. 4. We take  $(m_{\chi_2} - m_{\chi_1})/m_{\chi_1} = 0.01$ ,  $m_\psi = m_{\chi_2}$  and  $Y = 1$ . The extension of the allowed region compared with Fig. 2 is caused by coannihilation processes

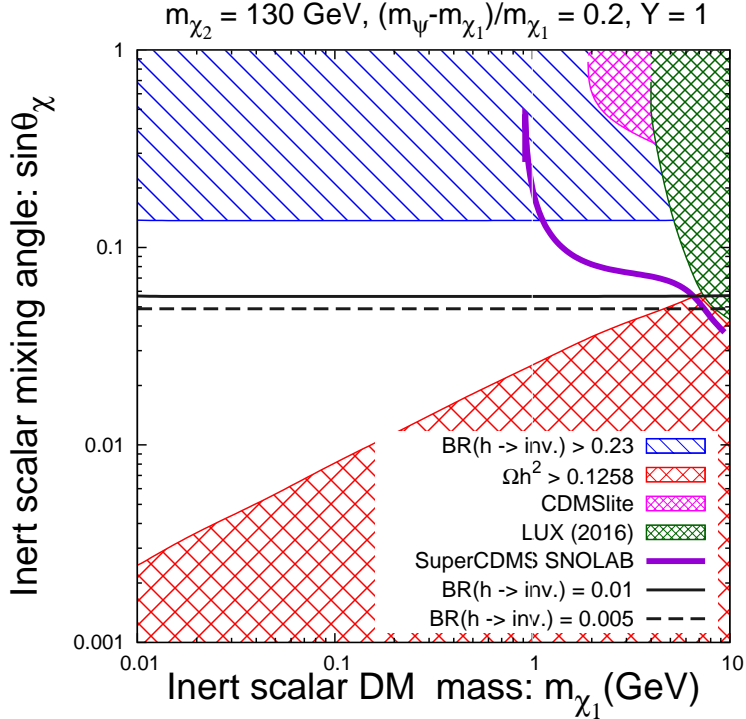


FIG. 3: Experimental constraints and future prospects in the  $(m_{\chi_1}, \sin \theta_\chi)$  plane in the model with a Majorana fermion for  $m_{\chi_2} = 130$  GeV,  $(m_\psi - m_{\chi_1})/m_{\chi_1} = 0.2$  and  $Y = 1$ .

mediated by  $\psi$ . The dominant coannihilation modes in this case are  $\eta^\pm \eta^\pm \rightarrow \tau^\pm \tau^\pm$ ,  $\chi_2^{(*)} \eta^\pm \rightarrow \bar{\nu} \tau^+(\nu \tau^-)$  and  $\chi_2^{(*)} \chi_2^{(*)} \rightarrow \nu \nu (\bar{\nu} \bar{\nu})$ , whose relative contributions to the effective annihilation cross section amount to around 75%. This allowed region is further investigated at XENON-1T [41].

## VI. CONCLUSIONS

We have investigated phenomenological implications of the complex scalar WIMP that is an admixture of an isospin doublet scalar and a complex singlet scalar. This class of model is naturally realized in SUSY models equipped with right-handed sneutrinos that have large trilinear scalar couplings. Due to a hypothetical global  $U(1)$  symmetry, the lighter mixed neutral scalar is stabilized, and thus become a WIMP. We have shown that there are two viable WIMP mass ranges where the WIMP abundance is consistent with the DM abundance:  $m_{\chi_1} \simeq m_h/2$  and  $m_{\chi_1} \gtrsim 100$  GeV. We have also pointed out that by introducing an additional isospin singlet Majorana fermion, the constraint from the dark matter abundance

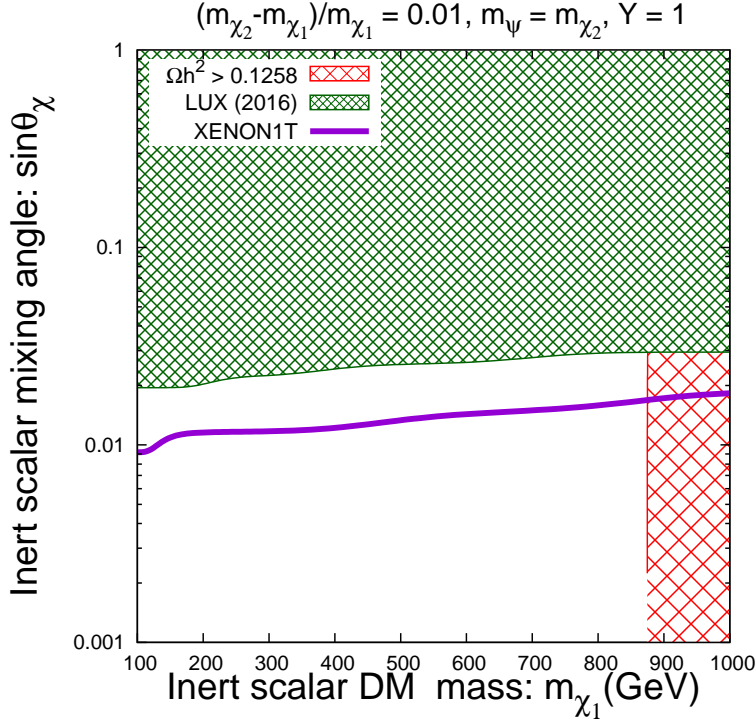


FIG. 4: Experimental constraints and future prospects in the  $(m_{\chi_2}, \sin \theta_\chi)$  plane in the model with a Majorana fermion for  $(m_{\chi_2} - m_{\chi_1})/m_{\chi_1} = 0.01$ ,  $m_\psi = m_{\chi_2}$  and  $Y = 1$ .

can be satisfied even when the mass of the WIMP is smaller than around 5 GeV. These cosmologically allowed regions can be further probed at upgraded DM detection experiments and future collider experiments.

### Acknowledgments

We thank Shinya Kanemura, Hiroaki Sugiyama and Koji Tsumura for valuable discussions and comments. This work was supported, in part, by Grant-in-Aid for Scientific Research on Innovative Areas, the Ministry of Education, Culture, Sports, Science and Technology, Nos. 16H01093 (M.K.) and 26105514 (O.S.), Grant-in-Aid for Scientific Research (C), Japan Society for the Promotion of Science, No. 26400243 (O.S.), the Sasakawa Scientific Research Grant from The Japan Science Society (A.S.), and by the SUHARA Memorial Foundation

(O.S.).

- 
- [1] G. Aad *et al.* [ATLAS Collaboration], Phys. Lett. B **716**, 1 (2012).
- [2] S. Chatrchyan *et al.* [CMS Collaboration], Phys. Lett. B **716**, 30 (2012).
- [3] G. Hinshaw *et al.* [WMAP Collaboration], Astrophys. J. Suppl. **208**, 19 (2013).
- [4] P. A. R. Ade *et al.* [Planck Collaboration], Astron. Astrophys. **571**, A16 (2014).
- [5] J. Brau, (Ed.) *et al.* [ILC Collaboration], arXiv:0712.1950 [physics.acc-ph]; G. Aarons *et al.* [ILC Collaboration], arXiv:0709.1893 [hep-ph]; N. Phinney, N. Toge and N. Walker, arXiv:0712.2361 [physics.acc-ph]; T. Behnke, (Ed.) *et al.* [ILC Collaboration], arXiv:0712.2356 [physics.ins-det]; T. Behnke *et al.*, arXiv:1306.6329 [physics.ins-det]; H. Baer, *et al.* "Physics at the International Linear Collider", *Physics Chapter of the ILC Detailed Baseline Design Report*: <http://lcsim.org/papers/DBDPhysics.pdf>.
- [6] D. M. Asner, T. Barklow, C. Calancha, K. Fujii, N. Graf, H. E. Haber, A. Ishikawa and S. Kanemura *et al.*, arXiv:1310.0763 [hep-ph].
- [7] G. Moortgat-Pick *et al.*, Eur. Phys. J. C **75**, no. 8, 371 (2015).
- [8] K. Fujii *et al.*, arXiv:1506.05992 [hep-ex].
- [9] E. Accomando *et al.* [CLIC Physics Working Group Collaboration], hep-ph/0412251; L. Linssen, A. Miyamoto, M. Stanitzki and H. Weerts, arXiv:1202.5940 [physics.ins-det].
- [10] M. Bicer *et al.* [TLEP Design Study Working Group Collaboration], JHEP **1401**, 164 (2014).
- [11] N. G. Deshpande and E. Ma, Phys. Rev. D **18**, 2574 (1978).
- [12] R. Barbieri, L. J. Hall and V. S. Rychkov, Phys. Rev. D **74**, 015007 (2006).
- [13] C. P. Burgess, M. Pospelov and T. ter Veldhuis, Nucl. Phys. B **619**, 709 (2001).
- [14] H. Davoudiasl, R. Kitano, T. Li and H. Murayama, Phys. Lett. B **609**, 117 (2005).
- [15] J. Goodman, M. Ibe, A. Rajaraman, W. Shepherd, T. M. P. Tait and H. B. Yu, Phys. Rev. D **82**, 116010 (2010).
- [16] C. Arina and N. Fornengo, JHEP **0711**, 029 (2007).
- [17] G. Belanger, K. Kannike, A. Pukhov and M. Raidal, JCAP **1204**, 010 (2012).
- [18] N. Arkani-Hamed, L. J. Hall, H. Murayama, D. Tucker-Smith and N. Weiner, Phys. Rev. D **64**, 115011 (2001).
- [19] G. Belanger, M. Kakizaki, E. K. Park, S. Kraml and A. Pukhov, JCAP **1011**, 017 (2010).



- [20] M. Kakizaki, E. K. Park, J. h. Park and A. Santa, Phys. Lett. B **749**, 44 (2015).
- [21] C. Arina, M. E. C. Catalan, S. Kraml, S. Kulkarni and U. Laa, JHEP **1505**, 142 (2015).
- [22] T. Cohen, J. Kearney, A. Pierce and D. Tucker-Smith, Phys. Rev. D **85**, 075003 (2012).
- [23] S. Banerjee, S. Matsumoto, K. Mukaida and Y. L. S. Tsai, JHEP **1611**, 070 (2016).
- [24] M. Kadastik, K. Kannike and M. Raidal, Phys. Rev. D **80**, 085020 (2009), Erratum: [Phys. Rev. D **81**, 029903 (2010)].
- [25] M. Kadastik, K. Kannike and M. Raidal, Phys. Rev. D **81**, 015002 (2010).
- [26] M. Kadastik, K. Kannike, A. Racioppi and M. Raidal, Phys. Lett. B **694**, 242 (2010).
- [27] C. Bonilla, D. Sokolowska, N. Darvishi, J. L. Diaz-Cruz and M. Krawczyk, J. Phys. G **43**, no. 6, 065001 (2016).
- [28] D. S. Akerib *et al.* [LUX Collaboration], Phys. Rev. Lett. **116**, no. 16, 161301 (2016).
- [29] D. S. Akerib *et al.*, arXiv:1608.07648 [astro-ph.CO].
- [30] R. Agnese *et al.* [SuperCDMS Collaboration], Phys. Rev. Lett. **116**, no. 7, 071301 (2016).
- [31] M. Ackermann *et al.* [Fermi-LAT Collaboration], Phys. Rev. D **89**, 042001 (2014).
- [32] M. Ackermann *et al.* [Fermi-LAT Collaboration], Phys. Rev. Lett. **115**, no. 23, 231301 (2015).
- [33] R. Caputo, M. R. Buckley, P. Martin, E. Charles, A. M. Brooks, A. Drlica-Wagner, J. M. Gaskins and M. Wood, Phys. Rev. D **93**, no. 6, 062004 (2016).
- [34] S. Schael *et al.* Phys. Rept. **427**, 257 (2006).
- [35] G. Aad *et al.* [ATLAS Collaboration], JHEP **1511**, 206 (2015).
- [36] S. Chatrchyan *et al.* [CMS Collaboration], Eur. Phys. J. C **74**, 2980 (2014).
- [37] K. Choi *et al.* [Super-Kamiokande Collaboration], Phys. Rev. Lett. **114**, no. 14, 141301 (2015).
- [38] A. Semenov, Comput. Phys. Commun. **180**, 431 (2009); Comput. Phys. Commun. **201**, 167 (2016).
- [39] G. Belanger, F. Boudjema, A. Pukhov and A. Semenov, Comput. Phys. Commun. **185**, 960 (2014).
- [40] A. Belyaev, N. D. Christensen and A. Pukhov, Comput. Phys. Commun. **184**, 1729 (2013).
- [41] E. Aprile *et al.* [XENON Collaboration], JCAP **1604**, no. 04, 027 (2016).
- [42] LEP SUSY Working Group (ALEPH, DELPHI, L3, OPAL), <http://lepsusy.web.cern.ch/lepsusy/Welcome.html>.
- [43] G. Aad *et al.* [ATLAS Collaboration], JHEP **1405**, 071 (2014).
- [44] V. Khachatryan *et al.* [CMS Collaboration], Eur. Phys. J. C **74**, no. 9, 3036 (2014).

- [45] G. Aad *et al.* [ATLAS Collaboration], JHEP **1410**, 96 (2014).
- [46] P. Cushman *et al.*, arXiv:1310.8327 [hep-ex].
- [47] A. Ishikawa, Talk at the 16th International Workshop on Future Linear Collider (LCWS14), Belgrade, Serbia, October 6-10, 2014.